

On-Pathway Oligomer of Human Islet Amyloid Polypeptide Induced and Stabilized by Mechanical Rotation during Magic Angle Spinning Nuclear Magnetic Resonance

Samuel D. McCalpin, Malitha C. Dickwella Widanage, Riqiang Fu, and Ayyalusamy Ramamoorthy*



Cite This: *J. Phys. Chem. Lett.* 2023, 14, 7644–7649



Read Online

ACCESS |



Metrics & More

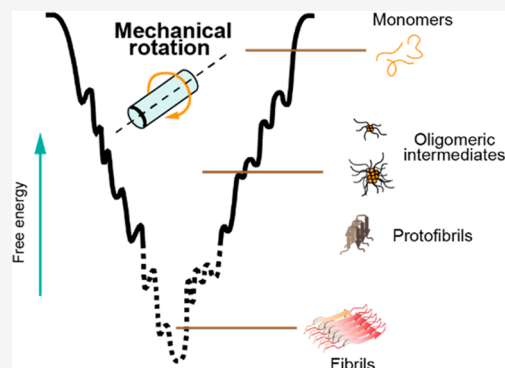


Article Recommendations



Supporting Information

ABSTRACT: Intermediates along the fibrillation pathway are generally considered to be the toxic species responsible for the pathologies of amyloid diseases. However, structural studies of these species have been hampered by heterogeneity and poor stability under standard aqueous conditions. Here, we report a novel methodology for producing stable, on-pathway oligomers of the human type-2 diabetes-associated islet amyloid polypeptide (hIAPP or amylin) using the mechanical forces associated with magic angle spinning (MAS). The species were a heterogeneous mixture of globular and short rod-like species with significant β -sheet content and the capability of seeding hIAPP fibrillation. We used MAS nuclear magnetic resonance to demonstrate that the nature of the species was sensitive to sample conditions, including peptide concentration, ionic strength, and buffer. The methodology should be suitable for studies of other aggregating systems.



Several degenerative diseases, including Alzheimer's disease (AD), Parkinson's disease (PD), and type-2 diabetes (T2D), are linked to the aggregation of proteins and peptides into fibrillar structures called amyloid.^{1–4} While the relationship between amyloid aggregation and these diseases has been established several decades ago, few successful treatments have been developed that target the fibril formation process.⁵ Structural biologists seeking to guide drug design struggle to characterize amyloid fibrils because their large size and noncrystalline nature render traditional solution nuclear magnetic resonance (NMR) and crystallography unfeasible. Still, solid-state NMR and cryogenic electron microscopy (cryo-EM) have proven to be capable of revealing specific, atom-resolution cross- β -sheet structures in fibril cores. However, recent research indicates that intermediate aggregates along the amyloid formation pathway, called “oligomers” or “protofibrils” based on size and morphology, are the toxic species most responsible for the pathologies of AD, PD, T2D, and other amyloidoses.^{6–9} Structural characterizations of oligomeric amyloid aggregates would greatly benefit efforts to develop treatments against amyloid diseases, but several factors have made them scarce, if not non-existent. The most significant factors are high heterogeneity among oligomeric species and their short lifetimes under aqueous conditions.

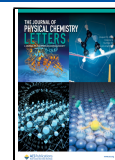
Magic angle spinning (MAS) solid-state NMR spectroscopy is uniquely positioned to characterize heterogeneous systems of intermediate molecular weight, slow-tumbling species, such as amyloid oligomers. Its sensitivity to individual nuclei in distinct chemical environments allows for discrimination

between differently structured conformers. Additionally, a combination of a dipolar recoupling experiment and intermediate frequency MAS has been demonstrated to facilitate the separation of the oligomer signal from that of monomers and fibrils in a heterogeneous preparation of amyloid- β .¹⁰ Typically, MAS experiments require biological samples to be lyophilized, frozen, or crystallized, but comprehensive multiphase (CMP) NMR spectroscopy enables the direct observation of mixed-phase systems with liquids.¹¹ The technique has been used to study microorganisms and environmental samples but also presents an approach to characterize heterogeneous amyloid systems consisting of soluble fast-tumbling monomers and low-order oligomeric aggregates and insoluble slow-tumbling high-order oligomers and fibrillar aggregates. The significant mechanical forces, such as centrifugal pressure, involved in MAS additionally offer a novel modulator of the amyloid formation pathway. Previous work has demonstrated the ability of small molecules, peptides, lipid membranes, metals, synthetic polymers, pH, and electric fields to alter amyloid aggregation pathways and in some cases to stabilize oligomeric intermediates for further structural studies.^{12–24} Pressure as a result of centrifugal forces during

Received: July 19, 2023

Accepted: August 16, 2023

Published: August 21, 2023



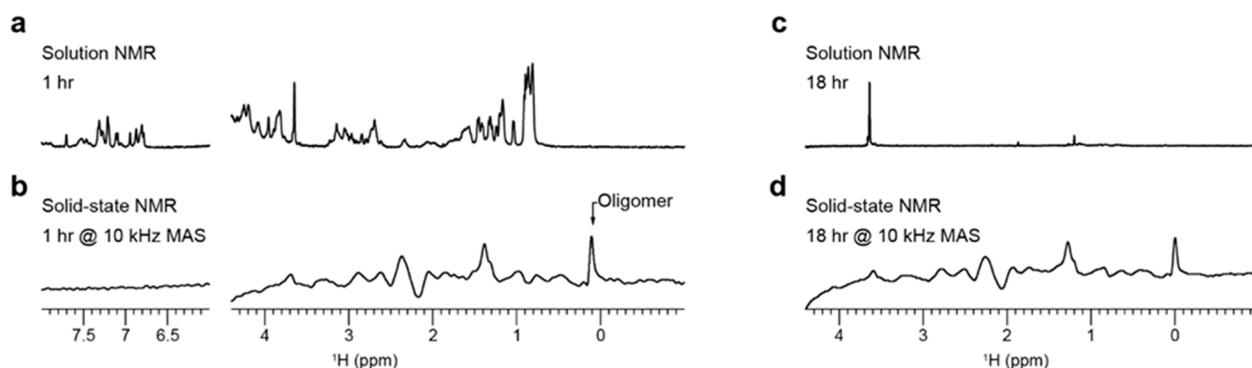


Figure 1. Visualizing the peaks of the oligomeric intermediate under MAS. hIAPP monomers were detected from (a and c) solution NMR and (b and d) MAS NMR using ^1H spectra obtained at 1 and 18 h time points on a 500 MHz spectrometer at 298 K. Both samples contained $50\ \mu\text{M}$ hIAPP in 10 mM d_{11} -Tris and 100 mM NaCl at pH 7.4 buffer.

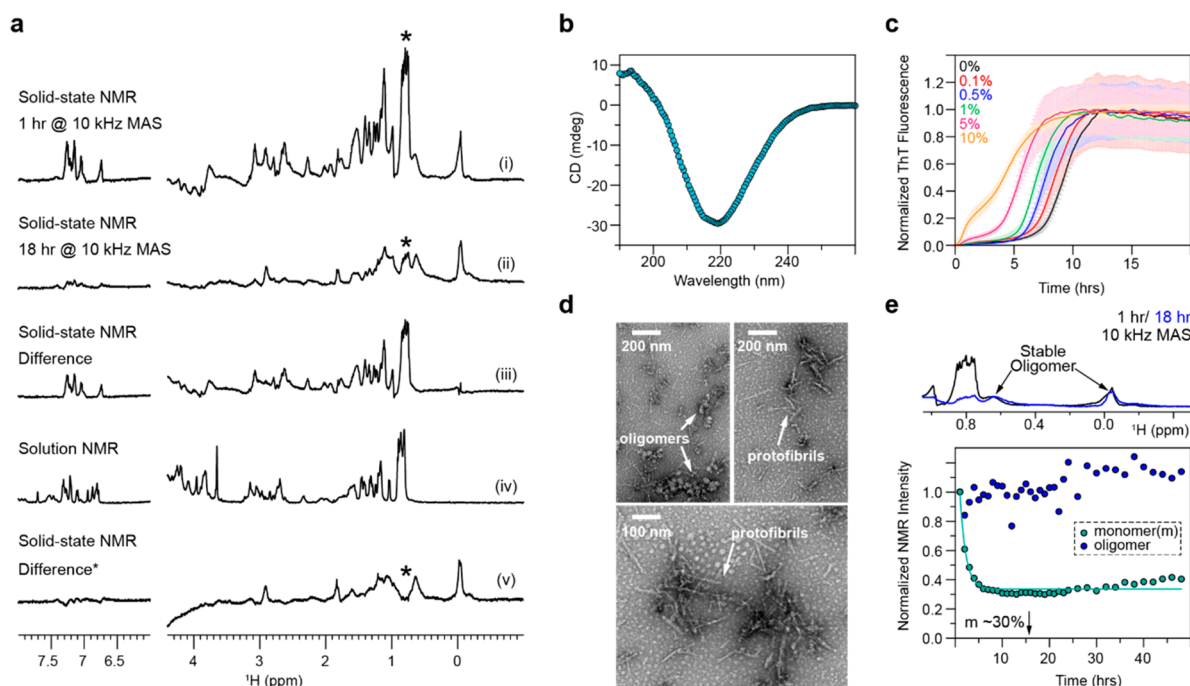


Figure 2. Heterogeneous, β -sheet structured, on-pathway hIAPP oligomers induced by MAS. (a) 1D ^1H NMR spectra with spectral editing showing the MAS-hIAPP oligomeric intermediates: (i) after 1 h, (ii) after 18 h, (iii) difference spectrum of spectra i and ii (normalized by the number of scans), (iv) solution NMR spectrum of hIAPP, and (v) difference spectrum of spectra ii and i (normalized by the peak with an asterisk). (b) β -Sheet structure was identified using CD spectroscopy. (c) ThT fluorescence assay of hIAPP monomers with noted concentrations of MAS-hIAPP seeds. (d) TEM revealed heterogeneous MAS-hIAPP species; oligomers and protofibrils are labeled in images taken from one sample at three different positions on the grid. (e) Normalized intensities from 1 to 0.5 ppm (represent monomers) and from 0.2 to -0.3 ppm (represent oligomeric intermediates) in 1D ^1H spectra show that monomers are depleted up to 30% while formed oligomeric intermediates are stable. For MAS NMR, 80 nmol of hIAPP was hydrated to 2 mM in D_2O . NMR data were collected over 48 h with 10 kHz MAS, and then the sample was removed from the rotor for further characterization. The MAS-hIAPP was diluted to $80\ \mu\text{M}$ in D_2O for CD spectroscopy, $100\ \mu\text{M}$ for TEM, and noted molar ratios relative to $5\ \mu\text{M}$ monomeric hIAPP in sodium phosphate buffer (10 mM NaPO_4 , 100 mM NaCl, and 10 mM ThT at pH 7.4) for ThT experiments.

MAS has been found to affect the structure and dynamics of bacteriorhodopsins and apoferritin, but its effect on the species formed during amyloid aggregation has not been fully characterized.^{25–27} Here, we provide the first report, to the best of our knowledge, of the ability of the mechanical forces associated with MAS to stabilize intermediate, on-pathway aggregates of human islet amyloid polypeptide (hIAPP) in an aqueous environment.

To compare the aggregation behavior of hIAPP with and without MAS, we prepared two samples and collected ^1H NMR spectra over the course of 24 h using a standard static

solution probe and a CMP probe with 10 kHz MAS (Figure 1). The sample conditions were identical except for 100% D_2O used in the MAS sample compared to 10% D_2O used in the solution NMR sample. Under the conditions of the solution NMR experiment, the ^1H NMR spectrum of hIAPP appeared with the line shape in Figure 1a, and the signal quickly decayed as the peptide aggregated within 7–8 h. This loss of signal is typical of aggregating peptides, because the signal broadens without MAS as the peptide complexes increase in size. In contrast, the MAS sample immediately afforded a much broader line shape with a significant peak near 0 ppm (Figure

1b). A peak at 0 ppm has been previously reported and characterized as arising from solvent-protected aliphatic protons in oligomeric aggregates of amyloidogenic peptides; therefore, we assigned this peak as belonging to an oligomeric species of hIAPP.^{10,28–30} This signal was also stable for at least 24 h (Figure 1d). To rule out D₂O as the cause of the differences between the samples, we performed a thioflavin T (ThT) fluorescence assay with buffers of varying amounts of D₂O and observed no change in the kinetics based on the percentage of D₂O (Figure S1 of the Supporting Information). Thus, our data suggest that MAS induced the formation of a hIAPP aggregate.

However, as a result of the smaller volume of the MAS rotor, significantly less material was present in the MAS experiment than in the solution experiment, causing a noisier signal. There was also notable baseline rolling in the MAS spectrum, which we hypothesized arose from conductivity through the coil as a result of salt in the buffer. To address these issues, we performed the MAS experiment again using a sample with a higher concentration of hIAPP in pure D₂O (Figure 2a). Interestingly, the aggregation behavior of this sample, as assessed by a series of ¹H NMR spectra collected under 10 kHz MAS, differed greatly from that of the previous sample. In this case, the ¹H NMR line shape was initially much sharper and decayed over time to a broader, less intense line shape, which was stable after 18 h. Subtracting the spectrum at 18 h from the initial spectrum revealed a line shape that was remarkably similar to that of the solution spectrum, suggesting that the spectral changes over time resulting from the depletion of hIAPP monomers as they associated into larger species. Additionally, we subtracted the solution spectrum from the long-time MAS spectrum, normalized to the intensity of the peak at 0.95 ppm, to obtain the line shape of the hIAPP aggregates. The presence of a peak near 0 ppm, which did not vary with time, suggested that these species (denoted as MAS-hIAPP) were formed immediately under MAS and were stable for at least 24 h.

We then characterized the MAS-hIAPP by a combination of fluorescence, circular dichroism (CD) spectroscopy, and transmission electron microscopy (TEM). CD exhibited a strong negative peak at 218 nm, indicative of a significant β -sheet content (Figure 2b). The ThT fluorescence assay showed sigmoidal aggregation kinetics for hIAPP monomers in the presence of seeds taken from the MAS sample. In contrast, the fluorescence intensity of ThT in the presence of the MAS aggregate alone was constant over time and noticeably less than that of the monomers that formed fibrils (Figure S2 of the Supporting Information). Lag times of monomer aggregation decreased with increasing concentrations of MAS-hIAPP seeds, demonstrating that MAS-hIAPP seeded aggregation of hIAPP monomers. Taken together, these results indicate that MAS induced the formation of on-pathway hIAPP oligomers with significant β -sheet content. However, TEM revealed a mixture of morphologies, including amorphous globular aggregates and rod-like protofibrillar species, which were much shorter than the fibers formed by hIAPP under static conditions (Figure 2d and Figure S3 of the Supporting Information). On the basis of the data presented here, we cannot determine whether one or both observed species are on-pathway. However, it seems most likely that the smaller globular aggregates were the dominant contributors to the NMR and CD spectra, assuming their faster tumbling and greater aqueous solubility. Regardless, the data confirm that

MAS induced the formation of non-fibrillar oligomeric intermediates of hIAPP.

There were issues reproducing the MAS-hIAPP formation in D₂O (Figure S4 of the Supporting Information), perhaps as a result of the use of an unbuffered solvent. Solution pH has been extensively reported to affect the kinetics of hIAPP aggregation and the end species formed, and solution conditions have been generally found to influence amyloid polymorphism; therefore, it is favorable to control these conditions regardless of any issues with reproducibility.^{31–36} To this end, we prepared hIAPP samples in several buffer conditions and collected ¹H MAS spectra as before. The observed ¹H lineshapes for each sample condition were compiled in Figure 3. In all cases, there was a peak near 0

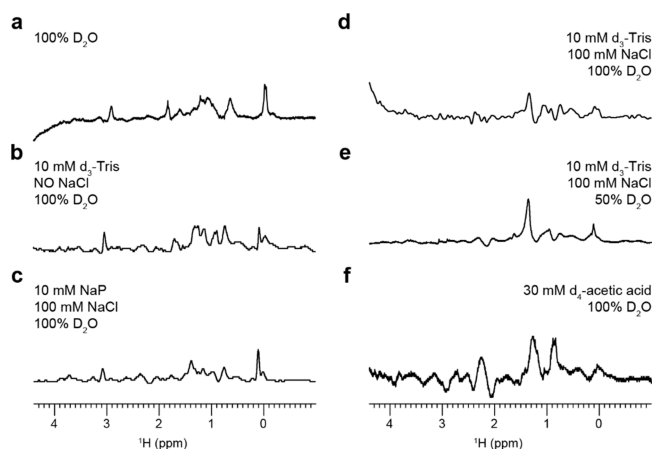


Figure 3. MAS-induced aggregation pathway altered by buffer. Solution conditions modified hIAPP aggregation under 10 kHz MAS. hIAPP concentrations are (a) 2 mM, (b) 2 mM (pH 7.4), (c) 2 mM (pH 7.4), (d) 2 mM (pH 7.4), (e) 50 μ M (pH 7.4), and (f) 50 μ M (pH 5.5). A 0 ppm peak indicated the presence of oligomeric intermediates.

ppm at the initial time point which did not significantly change for at least 18 h, consistent with the immediate formation of a stable oligomer regardless of buffer. The 0 ppm peak was weakest for the low hIAPP concentration, acetate buffer condition, which is unsurprising given that both a low peptide concentration and low pH are known to reduce hIAPP aggregation (Figure 3f).^{32,37} Remarkably, although there was significant spectral variation across the samples, the lineshapes reported for the oligomers formed in 2 mM hIAPP in pure D₂O, Tris buffer (no salt), and sodium phosphate buffer (with salt) were very similar (panels a–c of Figure 3). This suggests that a similar species or range of species formed under these sample conditions. On the basis of the differences between the spectral patterns of panels d and e of Figure 3 and between panels a, b, and d of Figure 3, the peptide concentration and buffer ionic strength seemed to be the most significant factors that influenced the nature of the oligomers formed. Tris also appeared to interact with hIAPP and bias the aggregation pathway but only in the presence of salt.

The amount of structural information that we could obtain from one-dimensional (1D) ¹H NMR lineshapes was limited; therefore, we collected two-dimensional (2D) ¹H–¹H radio-frequency-driven recoupling (RFDR) MAS spectra of a MAS-hIAPP sample in pure D₂O (Figure 4).³⁸ These RFDR spectra (Figure 4a) exhibited several well-resolved cross-peaks mostly saturated with 25 ms mixing (Figure 4c and Figure S5 of the

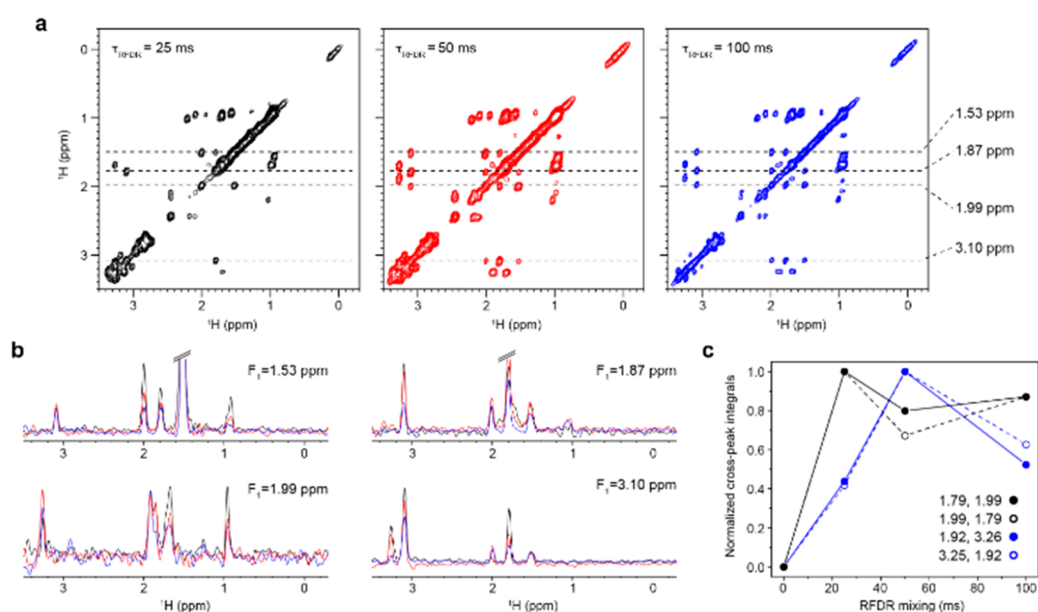


Figure 4. Dipolar recoupling from MAS-hIAPP. 2D ^1H – ^1H RFDR spectra of 2 mM hIAPP in 100% D_2O were obtained with an 800 MHz NMR spectrometer under 15 kHz MAS at 298 K. (a) Obtained at three mixing times. (b) 1D slices and (c) buildup curves are plotted for the cross-peaks at the noted chemical shifts.

Supporting Information). A comparable spectrum of MAS-hIAPP in buffer (Figure S6 of the Supporting Information) displayed significantly fewer (but still well-resolved) cross-peaks. Considering that the primary difference between these two samples was a significant monomer population present in pure D_2O and not in buffer, the extra cross-peaks in the spectrum of the D_2O sample likely arose from this population. It seems unlikely that dipolar recoupling would occur so efficiently in small, fast-tumbling monomers; therefore, it is also possible that the observed cross-peaks represented low-order oligomers or monomers that were motionally restricted by transient interactions with larger, invisible oligomers. Regardless, the RFDR spectra demonstrated that MAS-hIAPP samples should be amenable to structural studies. Challenges related to peak assignments could be overcome in the future with three-dimensional (3D) heteronuclear experiments on ^{13}C -labeled peptides, and higher MAS frequency could allow for full observation of the larger oligomers.

Drug design efforts against amyloid diseases would greatly benefit from the structural studies of intermediate amyloid aggregates. Here, we presented a novel method to stabilize nonfibrillar species of hIAPP using the mechanical forces associated with MAS. On the basis of our data, we cannot definitively determine a mechanism for the stabilization of an aggregation intermediate, but it is likely that the centrifugal pressure associated with MAS altered the folding energy phase diagram. Pressure has long been known to influence protein structures, usually by causing full or partial denaturation, and has been used to study the folding process.³⁹ It is possible that the pressure experienced by hIAPP partially inhibited the folding associated with its aggregation such that it could not progress past a partially folded intermediate. A pressure-stabilized folding intermediate of ubiquitin was described previously and might provide a useful analogy to the situation observed here.⁴⁰ In any case, we showed that the heterogeneous mixture of species included rod-like protofibrils and globular aggregates and on-pathway, β -sheet-rich species that formed within several hours in pure D_2O or immediately

in common buffer conditions. The sample conditions, namely, the peptide concentration and choice of buffer, were also found to affect the oligomers formed. 2D RFDR experiments showed that the MAS-hIAPP was amenable to further structural characterization. Such studies would deepen our understanding of the molecular basis of T2D. However, their feasibility in our hands was limited by the availability of the isotope-labeled peptide and MAS limits on liquid samples. Significantly, the methodology reported here should be broadly applicable to studying aggregates of other amyloidogenic peptides and intrinsically disordered proteins/peptides (IDPs) and is more tunable than chemical chaperones of oligomeric aggregates.

Experimental Methods. *Materials.* Synthetic, amidated human IAPP was purchased from Anaspec, treated with hexafluoroisopropanol (HFIP) for 1 h at room temperature, lyophilized, and stored at $-20\text{ }^\circ\text{C}$ prior to use. All other chemicals were obtained from Sigma-Aldrich.

MAS NMR. For MAS NMR at 500 MHz, 80 nmol of human islet amyloid polypeptide (hIAPP) was dissolved in HFIP and lyophilized directly into a 4 mm (outer diameter) KF MAS rotor insert. The peptide was hydrated in 40 μL of solvent; the rotor insert was inserted in a 4 mm rotor, of which both display no signal in ^1H NMR; and experiments were performed on a Bruker 500 MHz (11.7 T) spectrometer using a 4 mm comprehensive multiphase (CMP), triple-resonance HCN probe under 10 kHz MAS at 298 K. The radio-frequency field strengths were 55.5 kHz for ^1H hard pulse used for excitation. Sample conditions are specified in each figure caption.

The ^1H – ^1H RFDR spectra were recorded on a midbore 800 MHz (18.8 T) NMR spectrometer equipped with a Bruker NEO console using a 3.2 mm homemade triple-resonance HXY MAS probe. Samples were prepared as above, and 20 μL was transferred into a 3.2 mm rotor. The sample spinning rate was controlled by a Bruker pneumatic MASIII unit at 15 kHz \pm 5 Hz, and the sample temperature was set to 298 K. The ^1H 90° pulse length used in the experiments was 4.0 μs . States–time proportional phase incrementation (TPPI) was used for

quadrature detection in the t_1 dimension, and a ^1H 180° pulse was applied in the middle of each rotor period during the RFDR mixing time. The number of the rotor periods was adjusted to achieve various RFDR mixing times. The acquisition times for t_1 and t_2 dimensions were 25.6 and 61.44 ms, respectively. The data were zero-filled to a 4096×2048 matrix before Fourier transform and were processed with a Gaussian window function (LB = -20 Hz and GB = 0.1) in both dimensions.

Solution NMR. ^1H NMR spectra of hIAPP (50 μM in 10 mM d_{11} -Tris, 100 mM NaCl, and 10% D_2O for locking at pH 7.4 buffer) were collected on a 500 MHz Bruker NMR spectrometer using a triple-resonance TX1 probe. Spectra are presented as an average of 1024 scans collected with a 13 μs 90° pulse and a 3 s recycle delay.

TEM. After 48 h of spinning at 10 kHz, hIAPP (2 mM, 100% D_2O) was removed from the NMR rotor and diluted to a final concentration of 100 μM in D_2O . For TEM, 5 μL of the hIAPP sample was blotted on a carbon holey-mesh grid, and the grid was stained with 10 μL of 2% uranyl acetate. Images were collected on JEOL TEM.

CD Experiments. The MAS NMR hIAPP sample in 100% D_2O was diluted to 80 μM in D_2O , and its CD spectrum was measured in a JASCO CD spectropolarimeter using an average of 10 accumulations with 1 nm bandwidth, 0.5 nm data pitch, 100 nm/min scanning speed, 1 s data integration time, and 200 mdeg CD scale.

Seeding Experiments. The hIAPP in 100% D_2O sample was collected after solid-state NMR experiments (48 h of 10 kHz MAS) and diluted in D_2O . These MAS hIAPP species were mixed in several molar ratios with freshly prepared monomeric hIAPP (5 μM) and ThT (10 μM) in sodium phosphate buffer (10 mM NaPO_4 and 100 mM NaCl at pH 7.4). Samples (50 μL) were plated in quadruplicate in a black-walled, flat-bottomed 384-well microplate (Gruyner), and fluorescence emission at 480 nm was after excitation at 454 nm. The ThT fluorescence experiments were performed at 25 °C with measurements collected every 8 min.

■ ASSOCIATED CONTENT

SI Supporting Information

The Supporting Information is available free of charge at <https://pubs.acs.org/doi/10.1021/acs.jpcllett.3c02009>.

Methods and materials, additional ThT fluorescence, TEM, and MAS NMR data, and discussion of MAS NMR data reproducibility (PDF)

■ AUTHOR INFORMATION

Corresponding Author

Ayyalusamy Ramamoorthy – Biophysics Program, Department of Chemistry, Biomedical Engineering, Macromolecular Science and Engineering, Michigan Neuroscience Institute, University of Michigan, Ann Arbor, Michigan 48109, United States; Present Address: Ayyalusamy Ramamoorthy: National High Magnetic Field Laboratory, Department of Chemical and Biomedical Engineering, Florida State University, Tallahassee, Florida 32310, United States; orcid.org/0000-0003-1964-1900; Email: ramamoorthy@umich.edu, aramamoorthy@fsu.edu

Authors

Samuel D. McCalpin – Biophysics Program, Department of Chemistry, Biomedical Engineering, Macromolecular Science and Engineering, Michigan Neuroscience Institute, University of Michigan, Ann Arbor, Michigan 48109, United States

Malitha C. Dickwella Widanage – Biophysics Program, Department of Chemistry, Biomedical Engineering, Macromolecular Science and Engineering, Michigan Neuroscience Institute, University of Michigan, Ann Arbor, Michigan 48109, United States

Riqiang Fu – National High Magnetic Field Laboratory, Florida State University, Tallahassee, Florida 32310, United States; orcid.org/0000-0003-0075-0410

Complete contact information is available at:

<https://pubs.acs.org/doi/10.1021/acs.jpcllett.3c02009>

Notes

The authors declare no competing financial interest.

■ ACKNOWLEDGMENTS

This work was supported by the National Institutes of Health (NIH) Grant R01DK132214 (to A.R.). A portion of this work was performed at the National High Magnetic Field Laboratory, which is supported by the National Science Foundation Cooperative Agreement DMR-2128556 and the State of Florida.

■ REFERENCES

- (1) Knowles, T. P. J.; Vendruscolo, M.; Dobson, C. M. The Amyloid State and Its Association with Protein Misfolding Diseases. *Nat. Rev. Mol. Cell Biol.* **2014**, *15* (6), 384–396.
- (2) Hampel, H.; Hardy, J.; Blennow, K.; Chen, C.; Perry, G.; Kim, S. H.; Villemagne, V. L.; Aisen, P.; Vendruscolo, M.; Iwatsubo, T.; Masters, C. L.; Cho, M.; Lannfelt, L.; Cummings, J. L.; Vergallo, A. The Amyloid- β Pathway in Alzheimer's Disease. *Mol. Psychiatry* **2021**, *26* (10), 5481–5503.
- (3) Milardi, D.; Gazit, E.; Radford, S. E.; Xu, Y.; Gallardo, R. U.; Caffisch, A.; Westermark, G. T.; Westermark, P.; Rosa, C. L.; Ramamoorthy, A. Proteostasis of Islet Amyloid Polypeptide: A Molecular Perspective of Risk Factors and Protective Strategies for Type II Diabetes. *Chem. Rev.* **2021**, *121* (3), 1845–1893.
- (4) Mehra, S.; Sahay, S.; Maji, S. K. α -Synuclein Misfolding and Aggregation: Implications in Parkinson's Disease Pathogenesis. *Biochim. Biophys. Acta, Proteins Proteomics* **2019**, *1867* (10), 890–908.
- (5) Doig, A. J.; del Castillo-Frias, M. P.; Berthoumieu, O.; Tarus, B.; Nascica-Labouze, J.; Sterpone, F.; Nguyen, P. H.; Hooper, N. M.; Faller, P.; Derreumaux, P. Why Is Research on Amyloid- β Failing to Give New Drugs for Alzheimer's Disease? *ACS Chem. Neurosci.* **2017**, *8* (7), 1435–1437.
- (6) Haataja, L.; Gurlo, T.; Huang, C. J.; Butler, P. C. Islet Amyloid in Type 2 Diabetes, and the Toxic Oligomer Hypothesis. *Endocr. Rev.* **2008**, *29* (3), 303–316.
- (7) Cline, E. N.; Bicca, M. A.; Viola, K. L.; Klein, W. L. The Amyloid- β Oligomer Hypothesis: Beginning of the Third Decade. *J. Alzheimer's Dis.* **2018**, *64* (s1), S567–S610.
- (8) Ono, K. The Oligomer Hypothesis in α -Synucleinopathy. *Neurochem. Res.* **2017**, *42* (12), 3362–3371.
- (9) Birol, M.; Kumar, S.; Rhoades, E.; Miranker, A. D. Conformational Switching within Dynamic Oligomers Underpins Toxic Gain-of-Function by Diabetes-Associated Amyloid. *Nat. Commun.* **2018**, *9* (1), 1312.
- (10) Kotler, S. A.; Brender, J. R.; Vivekanandan, S.; Suzuki, Y.; Yamamoto, K.; Monette, M.; Krishnamoorthy, J.; Walsh, P.; Cauble, M.; Holl, M. M. B.; Marsh, E. N. G.; Ramamoorthy, A. High-Resolution NMR Characterization of Low Abundance Oligomers of Amyloid- β without Purification. *Sci. Rep.* **2015**, *5* (1), 11811.

- (11) Courtier-Murias, D.; Farooq, H.; Masoom, H.; Botana, A.; Soong, R.; Longstaffe, J. G.; Simpson, M. J.; Maas, W. E.; Fey, M.; Andrew, B.; Struppe, J.; Hutchins, H.; Krishnamurthy, S.; Kumar, R.; Monette, M.; Stronks, H. J.; Hume, A.; Simpson, A. J. Comprehensive Multiphase NMR Spectroscopy: Basic Experimental Approaches to Differentiate Phases in Heterogeneous Samples. *J. Magn. Reson.* **2012**, *217*, 61–76.
- (12) Ahmad, B.; Winkelmann, J.; Tiribilli, B.; Chiti, F. Searching for Conditions to Form Stable Protein Oligomers with Amyloid-like Characteristics: The Unexplored Basic PH. *Biochim. Biophys. Acta, Proteins Proteomics* **2010**, *1804* (1), 223–234.
- (13) Lopez del Amo, J. M.; Fink, U.; Dasari, M.; Grelle, G.; Wanker, E. E.; Bieschke, J.; Reif, B. Structural Properties of EGCG-Induced, Nontoxic Alzheimer's Disease A β Oligomers. *J. Mol. Biol.* **2012**, *421* (4), 517–524.
- (14) Chang, Y.-J.; Chen, Y.-R. The Coexistence of an Equal Amount of Alzheimer's Amyloid- β 40 and 42 Forms Structurally Stable and Toxic Oligomers through a Distinct Pathway. *FEBS J.* **2014**, *281* (11), 2674–2687.
- (15) Nedumpully-Govindan, P.; Kakinen, A.; Pilkington, E. H.; Davis, T. P.; Chun Ke, P.; Ding, F. Stabilizing Off-Pathway Oligomers by Polyphenol Nanoassemblies for IAPP Aggregation Inhibition. *Sci. Rep.* **2016**, *6* (1), 19463.
- (16) Prade, E.; Barucker, C.; Sarkar, R.; Althoff-Ospelt, G.; Lopez del Amo, J. M.; Hossain, S.; Zhong, Y.; Multhaup, G.; Reif, B. Sulindac Sulfide Induces the Formation of Large Oligomeric Aggregates of the Alzheimer's Disease Amyloid- β Peptide Which Exhibit Reduced Neurotoxicity. *Biochemistry* **2016**, *55* (12), 1839–1849.
- (17) Jayaraman, S.; Gantz, D. L.; Haupt, C.; Gursky, O. Serum Amyloid A Forms Stable Oligomers That Disrupt Vesicles at Lysosomal PH and Contribute to the Pathogenesis of Reactive Amyloidosis. *Proc. Natl. Acad. Sci. U. S. A.* **2017**, *114* (32), E6507–E6515.
- (18) Rodriguez Camargo, D. C.; Korshavn, K. J.; Jussupow, A.; Raltchev, K.; Goricanec, D.; Fleisch, M.; Sarkar, R.; Xue, K.; Aichler, M.; Mettenleiter, G.; Walch, A. K.; Camilloni, C.; Hagn, F.; Reif, B.; Ramamoorthy, A. Stabilization and Structural Analysis of a Membrane-Associated HIAPP Aggregation Intermediate. *eLife* **2017**, *6*, e31226.
- (19) Saikia, J.; Pandey, G.; Sasidharan, S.; Antony, F.; Nemade, H. B.; Kumar, S.; Chaudhary, N.; Ramakrishnan, V. Electric Field Disruption of Amyloid Aggregation: Potential Noninvasive Therapy for Alzheimer's Disease. *ACS Chem. Neurosci.* **2019**, *10* (5), 2250–2262.
- (20) Ciudad, S.; Puig, E.; Botzanowski, T.; Meigooni, M.; Arango, A. S.; Do, J.; Mayzel, M.; Bayoumi, M.; Chaignepain, S.; Maglià, G.; Cianferani, S.; Orekhov, V.; Tajkhorshid, E.; Bardiaux, B.; Carulla, N. A β (1–42) Tetramer and Octamer Structures Reveal Edge Conductivity Pores as a Mechanism for Membrane Damage. *Nat. Commun.* **2020**, *11* (1), 3014.
- (21) Gao, Y.; Guo, C.; Watzlawik, J. O.; Randolph, P. S.; Lee, E. J.; Huang, D.; Stagg, S. M.; Zhou, H.-X.; Rosenberry, T. L.; Paravastu, A. K. Out-of-Register Parallel β -Sheets and Antiparallel β -Sheets Coexist in 150-kDa Oligomers Formed by Amyloid- β (1–42). *J. Mol. Biol.* **2020**, *432* (16), 4388–4407.
- (22) Cox, S. J.; Rodriguez Camargo, D. C.; Lee, Y.-H.; Dubini, R. C. A.; Rovó, P.; Ivanova, M. I.; Padmini, V.; Reif, B.; Ramamoorthy, A. Small Molecule Induced Toxic Human-IAPP Species Characterized by NMR. *Chem. Commun.* **2020**, *56* (86), 13129–13132.
- (23) Sahoo, B. R.; Souders, C. L.; Watanabe-Nakayama, T.; Deng, Z.; Linton, H.; Suladze, S.; Ivanova, M. I.; Reif, B.; Ando, T.; Martyniuk, C. J.; Ramamoorthy, A. Conformational Tuning of Amylin by Charged Styrene-Maleic-Acid Copolymers. *J. Mol. Biol.* **2022**, *434*, 167385.
- (24) Roy, D.; Maity, N. C.; Kumar, S.; Maity, A.; Ratha, B. N.; Biswas, R.; Maiti, N. C.; Mandal, A. K.; Bhunia, A. Modulatory Role of Copper on HIAPP Aggregation and Toxicity in Presence of Insulin. *Int. J. Biol. Macromol.* **2023**, *241*, No. 124470.
- (25) Kawamura, I.; Kihara, N.; Ohmine, M.; Nishimura, K.; Tuzi, S.; Saitō, H.; Naito, A. Solid-State NMR Studies of Two Backbone Conformations at Tyr185 as a Function of Retinal Configurations in the Dark, Light, and Pressure Adapted Bacteriorhodopsins. *J. Am. Chem. Soc.* **2007**, *129* (5), 1016–1017.
- (26) Kawamura, I.; Yamaguchi, S.; Nishikawa, H.; Tajima, K.; Horigome, M.; Tuzi, S.; Saitō, H.; Naito, A. Change in Local Dynamics of Bacteriorhodopsin with Retinal Isomerization under Pressure as Studied by Fast Magic Angle Spinning NMR. *Polym. J.* **2012**, *44* (8), 863–867.
- (27) Bertini, I.; Luchinat, C.; Parigi, G.; Ravera, E.; Reif, B.; Turano, P. Solid-State NMR of Proteins Sedimented by Ultracentrifugation. *Proc. Natl. Acad. Sci. U. S. A.* **2011**, *108* (26), 10396–10399.
- (28) Narayanan, S.; Reif, B. Characterization of Chemical Exchange between Soluble and Aggregated States of β -Amyloid by Solution-State NMR upon Variation of Salt Conditions. *Biochemistry* **2005**, *44* (5), 1444–1452.
- (29) Soong, R.; Brender, J. R.; Macdonald, P. M.; Ramamoorthy, A. Association of Highly Compact Type II Diabetes Related Islet Amyloid Polypeptide Intermediate Species at Physiological Temperature Revealed by Diffusion NMR Spectroscopy. *J. Am. Chem. Soc.* **2009**, *131* (20), 7079–7085.
- (30) Huang, R.; Vivekanandan, S.; Brender, J. R.; Abe, Y.; Naito, A.; Ramamoorthy, A. NMR Characterization of Monomeric and Oligomeric Conformations of Human Calcitonin and Its Interaction with EGCG. *J. Mol. Biol.* **2012**, *416* (1), 108–120.
- (31) Abedini, A.; Raleigh, D. P. The Role of His-18 in Amyloid Formation by Human Islet Amyloid Polypeptide. *Biochemistry* **2005**, *44* (49), 16284–16291.
- (32) Brender, J. R.; Hartman, K.; Nanga, R. P. R.; Popovych, N.; de la Salud Bea, R.; Vivekanandan, S.; Marsh, E. N. G.; Ramamoorthy, A. Role of Zinc in Human Islet Amyloid Polypeptide Aggregation. *J. Am. Chem. Soc.* **2010**, *132* (26), 8973–8983.
- (33) Khemtémourian, L.; Doménech, E.; Doux, J. P. F.; Koorengevel, M. C.; Killian, J. A. Low PH Acts as Inhibitor of Membrane Damage Induced by Human Islet Amyloid Polypeptide. *J. Am. Chem. Soc.* **2011**, *133* (39), 15598–15604.
- (34) Santos, J.; Iglesias, V.; Santos-Suárez, J.; Mangiagalli, M.; Brocca, S.; Pallarès, I.; Ventura, S. PH-Dependent Aggregation in Intrinsically Disordered Proteins Is Determined by Charge and Lipophilicity. *Cells* **2020**, *9* (1), 145.
- (35) Su, Y.; Sarell, C. J.; Eddy, M. T.; Debelouchina, G. T.; Andreas, L. B.; Pashley, C. L.; Radford, S. E.; Griffin, R. G. Secondary Structure in the Core of Amyloid Fibrils Formed from Human B2m and Its Truncated Variant Δ N6. *J. Am. Chem. Soc.* **2014**, *136* (17), 6313–6325.
- (36) Sarell, C. J.; Woods, L. A.; Su, Y.; Debelouchina, G. T.; Ashcroft, A. E.; Griffin, R. G.; Stockley, P. G.; Radford, S. E. Expanding the Repertoire of Amyloid Polymorphs by Co-Polymerization of Related Protein Precursors. *J. Biol. Chem.* **2013**, *288* (10), 7327–7337.
- (37) Wei, L.; Jiang, P.; Xu, W.; Li, H.; Zhang, H.; Yan, L.; Chan-Park, M. B.; Liu, X.-W.; Tang, K.; Mu, Y.; Pervushin, K. The Molecular Basis of Distinct Aggregation Pathways of Islet Amyloid Polypeptide. *J. Biol. Chem.* **2011**, *286* (8), 6291–6300.
- (38) Ramamoorthy, A.; Xu, J. 2D $^1\text{H}/^1\text{H}$ RFDR and NOESY NMR Experiments on a Membrane-Bound Antimicrobial Peptide Under Magic Angle Spinning. *J. Phys. Chem. B* **2013**, *117* (22), 6693–6700.
- (39) Roche, J.; Royer, C. A.; Roumestand, C. Monitoring Protein Folding through High Pressure NMR Spectroscopy. *Prog. Nucl. Magn. Reson. Spectrosc.* **2017**, *102–103*, 15–31.
- (40) Kitahara, R.; Akasaka, K. Close Identity of a Pressure-Stabilized Intermediate with a Kinetic Intermediate in Protein Folding. *Proc. Natl. Acad. Sci. U. S. A.* **2003**, *100* (6), 3167–3172.